

On determining uncertainties of magnetic resonance sounding estimated transmissivities for groundwater modeling

Troels Norvin Vilhelmsen¹, Steen Christensen¹, and Esben Auken¹

ABSTRACT

The nuclear magnetic resonance sounding (MRS) method is used increasingly as a tool for hydrological investigations. Compared to other geophysical methods, the advantage of MRS is that it is directly sensitive to the presence of water in the subsurface. Data interpretations can also be used to get information about the subsurface pore structures, which under special conditions can be related to hydraulic properties such as aquifer transmissivity. However, to broaden the usage of this information in hydrological modeling, the uncertainties related to these transmissivity estimates must be determined. Otherwise, properly balanced weights cannot be given to the prior information obtained from MRS transmissivity estimates as compared to the hydrological data sets when used for groundwater model calibration. We have developed a methodology to estimate the uncertainties of MRS-based transmissivity estimates. Compared to previous studies, the methodology is well defined, and it takes into account important factors such as the uncertainties of the hydraulically estimated transmissivities, the uncertainty of the correlation factor in the petrophysical relation, and the uncertainties and correlations of the geophysically estimated parameters. We have determined the correlations and uncertainties of the geophysical parameters using a linear and a nonlinear method, and we find that the results are comparable.

INTRODUCTION

Groundwater models are usually set up with a predefined internal structure or hydrostratigraphy that is defined on the basis of geologic information, geophysical data analysis, and prior knowledge of the area investigated. Within this structure, model parameteriza-

tion is defined such that the model parameters can be calibrated to provide a reasonable fit between the observation data set and the simulated equivalents. Normally, these data consist of hydrological observations comprising static or dynamic water levels observed in boreholes, stream flow discharge measurements, etc. As an integrated part of the model inversion (often called model calibration in the hydrological community), the uncertainty of these data sets is evaluated to secure balanced weighting between the data when calibrating the groundwater flow model parameters. Ideally, the weight matrix associated with the observation data set should equal the inverse of the observation error covariance matrix. The uncertainty (here represented by the weighting) of the data set has implications for the estimated parameters. Parameters informed only by uncertain observations will be estimated with less confidence than parameters informed by observations of low uncertainty. Parameters of groundwater flow models may also suffer from parameter correlation. One example of this is the strong positive correlation between estimates of recharge and transmissivity that is the typical outcome when a groundwater model is calibrated to hydraulic head data only (e.g., Anderson et al. [2015], pp. 79–80). In such a case, independent prior information on transmissivity could potentially reduce parameter correlation and parameter uncertainties, and thereby reduce the uncertainty of predictions later made by the calibrated model. In cases where multiple estimates of local transmissivity can be obtained within an aquifer system, important information can be obtained on aquifer heterogeneity. This information can be valuable when hydrological models are set up in a highly parameterized context (Hunt et al., 2007). This is often done to resolve aquifer heterogeneity. However, this heterogeneity can rarely be resolved properly using hydraulic heads and flows only. Two examples of highly parameterized groundwater model setups can be seen from Doherty (2003) and Fienen et al. (2009). It is likely that both of these model studies would have benefitted from having point estimates of aquifer transmissivity.

Several studies have documented magnetic resonance soundings (MRS) as a geophysical method that can support hydrological investigations. Compared to other geophysical methods, MRS has a

Manuscript received by the Editor 17 September 2015; revised manuscript received 14 January 2016; published online 23 May 2016.

¹Aarhus University, Department of Geoscience, Aarhus C, Denmark. E-mail: troels.norvin@geo.au.dk; sc@geo.au.dk; esben.auken@geo.au.dk.

© 2016 Society of Exploration Geophysicists. All rights reserved.

more direct relation to hydrological parameters such as storage/storativity (e.g., Lubczynski and Roy, 2007) and hydraulic conductivity/transmissivity (e.g., Legchenko et al., 2002) due to the direct sensitivity of the observed MRS signal to the presence of water in the subsurface. Potentially, estimates of local transmissivities (which is the focus in the present study) and storativities derived from MRS can be used for constraining parameter variations of groundwater models, such that these can be used more effectively as tools for decision support for groundwater and surface water management. It is outside the scope of this paper to discuss the MRS method itself, and for this, we therefore refer to the comprehensive MRS review papers by Legchenko and Valla (2002) or Behroozmand et al. (2015).

A key obstacle for usage of MRS in hydrological modeling is estimation of the uncertainty of the derived transmissivity estimates. References suggesting how uncertainty of transmissivity (or hydraulic conductivity) can be estimated from MRS are numerous (e.g., Legchenko et al., 2004; Chalikakis et al., 2008; Plata and Rubio, 2008; Boucher et al., 2009; Günther and Müller-Petke, 2012; Vilhelmsen et al., 2014) but the methods or their documentation are often incomplete. In some references, it is just stated that the uncertainty given for the MRS-estimated transmissivities takes into account the uncertainty of the MRS data, MRS parameters, and transmissivity estimates (Legchenko et al., 2004; Boucher et al., 2009), but the method is not documented or explained. Chalikakis et al. (2008) estimate the uncertainty of the MRS-based transmissivity estimates, but they only seem to take equivalent solutions into account. Uncertainties of effective hydraulic conductivity can be estimated using joint inversion between TEM, MRS, and aquifer test models (Vilhelmsen et al., 2014), but the methodology is tedious and remains to be documented for sites with multiple MRS and aquifer tests. Plata and Rubio (2008) provide a detailed analysis of the importance of the uncertainty of transmissivities estimated using hydrological methods, but they do not give a detailed description on how to take this uncertainty into account. One of the few studies documenting the methodology used for estimating MRS-based transmissivity uncertainties is the study of Günther and Müller-Petke (2012). However, they do not take into account the potential MRS parameter correlation between, e.g., layer thickness and water content, which may or may not be profound.

In the following, we suggest and demonstrate a consistent methodology for estimating the uncertainty of an MRS-based transmissivity. The methodology takes into account factors such as MRS data quality (noise level), the according covariance of MRS-derived parameter estimates, the uncertainty of estimated transmissivities from the hydrological investigations (T_{HYD}), and the uncertainty of the relationship between MRS parameters and T_{HYD} . The suggested methodology is simplified by using linearized approximations for parameter covariances. We demonstrate the validity of this simplification by a comparison with results obtained by non-linear analysis.

METHODS

Hydrological methods

As outlined previously, estimates of transmissivity or effective hydraulic conductivity are often of practical importance for hydrologists because they can provide important information about the variability or heterogeneity within an investigated aquifer. Often

the transmissivity is thought of as the hydraulic conductivity times the thickness of the aquifer. This is, however, not strictly correct because the hydraulic conductivity can vary significantly vertically and horizontally within an aquifer comprising varying types of deposits. Hydraulic conductivity is thereby an intrinsic property of the sediments in the aquifer. In cases where the aquifer is heterogeneous (which is often/always the case), the transmissivity of an aquifer is defined as (Bear [1988], p. 214)

$$T_{\text{HYD}} = k_{\text{eff}} * l; \quad k_{\text{eff}} = \frac{1}{l} \int_0^l k(z) dz, \quad (1)$$

where T_{HYD} is the aquifer transmissivity, k_{eff} is the effective horizontal hydraulic conductivity, l is the aquifer thickness, and $k(z)$ represents the vertically varying hydraulic conductivity. When performing hydraulic tests on aquifers to determine their properties, one can usually only estimate T_{HYD} , or k_{eff} within a depth interval, but not $k(z)$.

Estimates of transmissivity can be obtained by aquifer tests or slug tests. An aquifer test can be performed in several ways, but the most typical is to pump from a single well with constant rate while observing drawdown in the pumping well and/or in nearby observation wells. Aquifer transmissivity and storativity can be estimated by analysis of the drawdown observations. The observations can also provide important information about existence, type, and location of aquifer boundaries. For a more complete review of aquifer test analysis, we refer to Kruseman and de Ridder (2000).

The slug test is a more simple methodology to estimate hydraulic parameters of the aquifer. At the beginning of the test, the groundwater level in the well is increased or decreased instantaneously (often by dropping or extracting a solid slug/object into or from the well), and the resulting aquifer response is observed by measuring how the hydraulic head in the well falls back to its static level. The effective hydraulic conductivity within a depth interval can be estimated by analyzing this response. Butler (1998) gives a detailed description of how slug tests can be carried out, analyzed, and processed.

Slug test analysis

The slug test data collected for the field case presented later was analyzed using the KGS model solution (Butler [1998], pp. 94–99) for confined aquifers. Due to noninstantaneous insertion/extraction of the slug, the initial part of the measured curve was disturbed, and the data were, therefore, processed using the translation method (Butler [1998], p. 52). In total, 22 slug test data sets were collected in two boreholes using slugs of two different sizes.

Pumping test analysis

Due to the large areal influence of long duration aquifer tests, the analysis of these can be more complex to interpret than slug tests. This is for example the case when geologic or hydrological boundaries influence on the drawdown response. In the field case presented later, the pumped aquifer is located in a buried valley structure incised into a low permeable substratum, and there are internal boundaries inside the valley as well. Methods to analyze aquifer tests performed in such valley structures have been given by,

e.g., Vandenberg (1977), or Butler and Wenzhi (1991), and in the presence of internal boundaries by van der Kamp and Maathuis (2012). However, the limitations of the analytical solutions make especially the Vandenberg solution inapplicable for the present analysis due to the long distance to some of the observation wells. The analysis presented by Butler and Wenzhi (1991) would likely be applicable to the present case, but due to their complicated solution, we found it easier to set up a simple numerical groundwater model to perform the analysis.

The numerical model was set up in MODFLOW2005 (Harbaugh, 2005), using one layer and a horizontal discretization of 10 m. The edges of the valley structure were applied as no flow boundaries, and the width and the thickness of the valley were assumed constant throughout the entire valley length. The aquifer system was simulated as confined with a constant transmissivity and storativity throughout the valley. To evaluate if the numerical discretization of the model was adequate, the numerical solution was compared to the analytical Theis solution (Theis, 1935) for drawdown in confined aquifers with infinite areal extent. After validation of the numerical resolution, we incorporated the valley into the model. The outlet of the valley was simulated as a constant head boundary conditions (BC) at a distance of 10 km from the pumping well. Increasing this distance further did not change the simulation results.

After setting up the numerical groundwater model, the parameters of the model were estimated by nonlinear regression using PEST (Doherty, 2010). Based on the optimized parameters, the parameter covariance matrix was determined as

$$C(\mathbf{p}) = \sigma^2 (\mathbf{X}^T \boldsymbol{\omega} \mathbf{X})^{-1}, \quad (2)$$

where \mathbf{X} is the Jacobian matrix for the optimized parameter set, $\boldsymbol{\omega}$ is the inverse of the observation error covariance matrix, and σ^2 is the reference variance determined as

$$\sigma^2 = \frac{\Phi}{m - n}, \quad (3)$$

where Φ is the objective function (equal to the sum of squared weighted misfit between the data and the modeled responses), n is the number of parameters, and m is the number of data points.

In the present analysis, the observation error covariance matrix for the drawdown observations was assumed to be diagonal and the standard error associated with the drawdown observation i was determined as

$$e_i = e_w + e_{\text{pct}} * d_i, \quad (4)$$

where e_w is the internal noise of the transducer and data logger used to monitor drawdown, e_{pct} is a scalar, and d_i is the observed drawdown. In this noise model, the first term accounts for measurement error, whereas the second term accounts for other error contributions such as error caused by simplifications of the applied model (model structural error, for example negligence in the model of aquifer heterogeneity). We, thus, expect model error to increase with drawdown. In the present analysis, e_w was determined to 0.01 m based on analysis of data collected just before initiation of the pumping test, and e_{pct} was set to 0.15 based on an analysis of data variability during the tests as well as on the expected effects of the model simplifications.

Geophysical methods

MRS uses the basic principle of nuclear magnetic resonance to excite the nuclei of the hydrogen protons found in the water molecules in the subsurface. This excitation is done by transmitting an alternating current tuned at the local Larmor frequency through a transmitter coil laid out on the surface. This creates a time-varying energizing magnetic field that tips the net magnetization vector of the hydrogen protons away from the alignment with the earth magnetic field. Once the energizing pulse has been terminated, the net magnetization vector relaxes back into equilibrium with the earth magnetic field. During this process, a signal is emitted, which can be measured in the receiver coil (e.g., Legchenko and Valla, 2002; Behroozmand et al., 2012b).

The simplest form of an MRS experiment uses a single excitation pulse and observes the following decay of the net magnetization back to equilibrium, also known as free induction decay (FID). Its envelope can be described by a monoexponential decay given by (Behroozmand et al., 2012b)

$$V(q, t) = \int K(q, z) w(z) \exp\left(-\frac{t}{T_2^*(z)}\right), \quad (5)$$

where $V(q, t)$ is the measured signal, $K(q, z)$ is the 1D kernel function, $w(z)$ is the water content as a function of depth (z), $T_2^*(z)$ is the relaxation rate including dephasing effects as a function of depth, and t is time after the pulse. The signal is dependent on the pulse moment (q), which is the product of the current amplitude and the pulse duration. By gradually increasing q , the sensitivity of the MRS experiment shifts to greater depth, thereby providing depth-related information.

The propagation of the used electromagnetic fields and thus the kernel $K(q, z)$ is dependent on the conductivity structure of the subsurface. This conductivity structure can be determined from a transient electromagnetic sounding (TEM) (Behroozmand et al., 2012a). Subsequently, the two data sets are jointly inverted determining layer thickness, resistivities, water content, and relaxation rate suggested by Behroozmand et al. (2012a). Forward responses for the TEM and MRS models were simulated using the algorithm AarhusInv (Auken et al., 2014), whereas the inversions were performed using PEST (Doherty, 2010). The uncertainties of the estimated parameters were determined using equation 2, where the data uncertainties were determined from the gated signal and by adding 3% of uniform noise.

The collected data sets for the field case presented later were processed using the methods described by Dalgaard (2014), Dalgaard et al. (2012), and Larsen et al. (2014). This includes despiking, coherent noise cancelation, stacking, and envelope detection.

Petrophysical relation

Under the assumption of fast diffusion, the permeability (k) of the subsurface can be determined from MRS using what is known as the Schlumberger-Doll Research equation presented by Kenyon et al. (1988) as (Dlugosch et al., 2013; Dlubac et al., 2014)

$$k = b * w^m * [T_2]^n, \quad (6)$$

where b is a correlation factor, w is the water content or effective porosity, T_2 is the transversal relaxation time, and m and n are

constants. For unconsolidated sediments, these constants are often set to 1 and 2, respectively (e.g., Legchenko et al., 2004). Because it can often be assumed that the density and viscosity of groundwater within the same region is constant, the hydraulic conductivity can be calculated from permeability by a simple linear transformation (Bear, 1988, p. 133). Moreover, in cases where the effects of magnetic field inhomogeneities can be neglected, the hydraulic conductivity can be estimated as

$$K_{\text{MRS}} = C_p * w * (T_2^*)^2, \quad (7)$$

where C_p is an empirical constant, most often determined by cross-correlation to effective hydraulic conductivity determined from pumping or slug or tests (K_{HYD}). Care should be taken when applying equation 7 to estimate K_{MRS} . In cases in which T_2^* is dominated by magnetic field inhomogeneities (e.g., due to magnetic materials in the subsurface), the relation between pore geometry and decay time deteriorates (Legchenko et al., 2002; Grunewald and Knight, 2011) and equation 7 becomes invalid.

For a vertically homogeneous aquifer with thickness l , the transmissivity (T_{MRS}) can be determined from equation 7 as

$$T_{\text{MRS}} = C_p * w * (T_2^*)^2 * l, \quad (8)$$

to facilitate the use of T_{MRS} in hydrological decision support, it is important to determine its reliability by estimating its uncertainty. The method to do so is described in the following.

First, equation 8 is log transformed (in the present, this refers to base 10) to give the linear equation

$$\log(T_{\text{MRS}}) = \log(C_p) + \log(w) + 2 * \log(T_2^*) + \log(l), \quad (9)$$

subsequently, by assuming that the $\log(C_p)$ estimate is independent from the other estimated terms used on the right side of the equation, the variance of $\log(T_{\text{MRS}})$ can be written as

$$\begin{aligned} \text{var}[\log(T_{\text{MRS}})] &= \text{var}[\log(C_p)] + \text{var}[\log(w)] \\ &+ 2 * \log(T_2^*) + \log(l), \end{aligned} \quad (10)$$

using basic probability theory, the variance related to the MRS-derived parameters can thus be determined as

$$\begin{aligned} \text{var}[\log(w) + 2 * \log(T_2^*) + \log(l)] &= \text{var}[\log(w)] + 4 * \text{var}[\log(T_2^*)] + \text{var}[\log(l)] \\ &+ 4 * \text{cov}[\log(w), \log(T_2^*)] \\ &+ 4 * \text{cov}[\log(T_2^*), \log(l)] + 2 * \text{cov}[\log(w), \log(l)], \end{aligned} \quad (11)$$

where $\text{var}[x]$ is the variance of x and $\text{cov}[x, y]$ is the covariance between x and y . In cases where correlation between the MRS-derived parameters is negligible, equation 11 simplifies to

$$\begin{aligned} \text{var}[\log(w) + 2 * \log(T_2^*) + \log(l)] &= \text{var}[\log(w)] + 4 * \text{var}[\log(T_2^*)] + \text{var}[\log(l)], \end{aligned} \quad (12)$$

the correlation constant $\log(C_p)$ and its associated uncertainty $\text{var}[\log(C_p)]$ can be determined from weighted linear regression

of equation 9 where T_{MRS} is substituted by T_{HYD} . The system of equations simplifies to

$$\log(C_p) = \frac{\sum_{i=1}^n \omega_i * y_i}{\sum_{i=1}^n \omega_i}, \quad (13)$$

where n refers to the number of equations (pairs of MRS and T_{HYD}). The weights (ω_i) associated with each equation in the linear regression is given by $1/(\text{var}[\log(w_i) + 2 * \log(T_{2i}^*) + \log(l_i)] + \text{var}[\log(T_{\text{HYD}i})])$, and y_i is given by $\log(T_{\text{HYD}i}) - [\log(w_i) + 2 * \log(T_{2i}^*) + \log(l_i)]$. By applying this methodology, it is secured that uncertain data sets are down weighted when determining C_p and that the uncertainty of the C_p factor can be taken into account when determining T_{MRS} . Subsequently, $\text{var}[\log(C_p)]$ can be determined for this simple case as (Aster et al., 2005)

$$\text{var}(\log(C_p)) = \left(\sum_{i=1}^n \omega_i \right)^{-1}, \quad (14)$$

to determine $\text{var}[T_{\text{MRS}}]$, the variance of T_{HYD} as well as the variance-covariance of the parameters pertaining to the MRS inversion these must be determined. This can be done from either the posterior linear analysis obtained from the MRS inversion using equation 2 (e.g., Behroozmand et al., 2012b) or through nonlinear analysis as described in the following.

Parameter variance estimation by nonlinear procedure

The nonlinear procedure has three steps:

- 1) Generate sets of parameters resulting in equivalent models as for the joint MRS/TEM setup.
- 2) Use these parameter sets to generate an estimate of the variance-covariance matrix for the geophysical parameters.
- 3) Use the element values of this estimated matrix in either equation (11) or (12) to calculate the variance related to the MRS-derived parameters.

In step 1, to generate parameter sets we applied a modified version of null-space Monte Carlo (NSMC) (Tonkin and Doherty, 2009). In this nonlinear approach, the inverted model for MRS is used to define the calibration null space. Based on the Jacobian matrix determined from the optimized MRS parameters (\mathbf{X}_{MRS}), the following equation can be determined through singular value decomposition,

$$\mathbf{X}_{\text{MRS}}^T \boldsymbol{\omega}_{\text{MRS}} \mathbf{X}_{\text{MRS}} = \mathbf{V} \mathbf{S} \mathbf{V}^T, \quad (15)$$

where $\boldsymbol{\omega}_{\text{MRS}}$ is the inverse of the MRS observation error covariance matrix, \mathbf{V} is a matrix of eigenvectors, and \mathbf{S} is a diagonal matrix containing the singular values arranged in decreasing order. In cases where the inversion of the MRS model is ill posed, some diagonal elements of \mathbf{S} are small (≈ 0), the $\mathbf{X}_{\text{MRS}}^T \boldsymbol{\omega}_{\text{MRS}} \mathbf{X}_{\text{MRS}}$ matrix is singular, and the inversion problem cannot be solved without applying some sort of regularization. In such cases, equation 15 can be written as

$$\mathbf{X}_{\text{MRS}}^T \boldsymbol{\omega}_{\text{MRS}} \mathbf{X}_{\text{MRS}} = [\mathbf{V}_p \quad \mathbf{V}_0] \begin{bmatrix} \mathbf{S}_p & 0 \\ 0 & \mathbf{S}_0 \end{bmatrix} [\mathbf{V}_p \quad \mathbf{V}_0]^T, \quad (16)$$

where V_p contains the eigenvectors spanning the solution space, V_0 contains the eigenvectors spanning the null space, and S_p and S_0 contains the singular values pertaining to the solution space and the null space, respectively. In the present case, we wish to use V_0 estimated from equation 16 to reduce the parameters space to be investigated to determine the contribution of model nonlinearity to parameter variance and covariance. According to Tonkin and Doherty (2009), this can be done by generating a set of realizations of random parameters p_{st} . This random parameter set could be generated using the posterior parameter covariance matrix $C(p)$. In the present case, this covariance matrix could be approximated by using the outcome of the linear analysis as described previously. However, because we seek to investigate the contribution from model nonlinearities to parameter uncertainties, selecting random parameters based on a linearized approximation of $C(p)$ could potentially result in underestimation of the uncertainty. Instead, we generated random parameter values within the 99% confidence intervals estimated by the linear analysis (p_{st}). A new parameter set that nearly fit the data (\hat{p}) can then be calculated as (Tonkin and Doherty, 2009)

$$(\hat{p} - p_{st})' = V_0 V_0^T (\hat{p} - p_{st}) \quad \bar{p} = \hat{p} + (\hat{p} - p_{st})', \quad (17)$$

where $V_0 V_0^T$ functions as a null-space projection matrix, and $(\hat{p} - p_{st})'$ is the null-space projection vector. Due to model nonlinearity, the parameter set (\bar{p}) generated by the null-space projection may not fit the calibration data set within the uncertainties of the conditioning data set. In this case, \bar{p} is slightly adjusted by performing up to a maximum of three inversion iterations. If the data are still not fitted within its uncertainty, the projected parameter set is rejected as nonbehavioral. In the present study, this process was repeated 2000 times for each MRS location. Parameter statistics was subsequently calculated based on the subset parameter combinations for each sounding resulting in behavioral models.

Because the MRS inversion problems in the present field case are all well posed, S does not have near-zero eigenvalues. However, in the context of Monte-Carlo analysis equation 17 can still be used to reduce to parameter space to be investigated. This is here done by selecting a truncation limit between S_p and S_0 such that S_p has $np/2$ diagonal elements, where np is the number of parameters in the inversion problem. This threshold was selected as a trade-off, where the aim was to reduce the number of iterations in the inversion of each set of parameters, while representing potential significant nonlinearities.

One of the challenges of applying this analysis is selecting the acceptable data fit resulting in behavioral models. In the present study, this is evaluated individually for each MRS by visual inspection of the fitted data curves from the linear analysis. The threshold was then set as a percentage above the minimum objective function obtained in the linear analysis. The percentage chosen was determined different for each sounding depending on the fit in the optimal model. Often this was in the order of 50% above the minimum objective function. This approach is similar to the one applied by Tonkin and Doherty (2009).

FIELD CASE

The suggested methodology to estimate MRS-based transmissivity uncertainties is demonstrated using a data set collected near a wellfield used by the water supply of Aarhus, Denmark (see Figure 1). The data set consists of five MRS, two aquifer tests, and slug

tests performed in two wells. The MRS data and the slug test data were collected during a field campaign in 2014, whereas the aquifer tests were conducted by the Danish consultant company NIRAS in 2002 (well: DGU78.860) and as a part of a master thesis project in 2006 (well: DGU78.343) (Blæsbjerg, 2006), respectively. A few details about the two pumping tests are given in Table 1.

The studied aquifer is located within a buried valley structure (Figure 1c), which is a part of a regional system of buried valleys found within the area outlined in Figure 1b (Jørgensen and Sander- sen, 2006; Møller et al., 2009). The valleys are incised into Paleogene clay, which acts as an impermeable bed of the deepest aquifer. The aquifers in the area primarily consist of meltwater deposits of sand and gravel. In areas with confined aquifers, aquitards are typically made up of clayey till and to a minor extent, lacustrine clay. The valley structures were primarily mapped using airborne TEM (Sørensen and Auken, 2004; Aarhus Geophysics, 2014), which have given detailed information about their extend. The MRS data sets were collected using Numis^{Poly} equipment from IRIS Instruments using 16 pulse moments, ranging from 0.073 to 8.39 As, and between 75–150 stacks. The number of stacks was chosen based on the local noise level. A 100 × 100 m square loop configuration was used to secure high-depth penetration.

RESULTS

Hydrological analysis

Figure 2 shows the observed and simulated drawdown responses for the two aquifer tests. Directly from the data, it is apparent that the aquifer is located in a valley structure, which gives the observed drawdown curves a characteristic straight-line shape in a log-log plot (Butler and Wenzhi, 1991). This shape has been observed from aquifer tests performed in similar structures elsewhere (e.g., van der Kamp and Maathuis, 2012).

The transmissivity is estimated to be 0.1374 m²/s for the DGU78.343 aquifer test, and 0.0871 m²/s for the DGU78.860 aquifer test, respectively. Some of the difference between the two estimates is due to uncertainties of the analysis. However, the primary explanation is likely to be a change in lithology to coarser sediments near DGU78.343. The uncertainties of the transmissivity estimates were determined using equation 2. This gave a log(T_{HYD}) standard deviation of 0.056 for the DGU78.343 determined transmissivity, and a log(T_{HYD}) standard deviation of 0.14 for the DGU78.860 determined transmissivity, respectively.

Figure 3 shows examples of the slug test data sets collected from two wells (DGU78.776 and DGU78.779) near Ristrup08 (see Figure 1). In total, 14 slug tests were performed in DGU78.776 and eight slug tests were performed in DGU 78.779. Due to the application of the translation method, the initial displacement of the

Table 1. Details on the performed aquifer tests.

Pumping well	Abstraction rate (m ³ /s)	Duration	Number of observation wells included in analysis
DGU78.860	0.04508	12 April–15 May, 2002	3
DGU78.343	0.01667	21 June–16 August, 2005	5

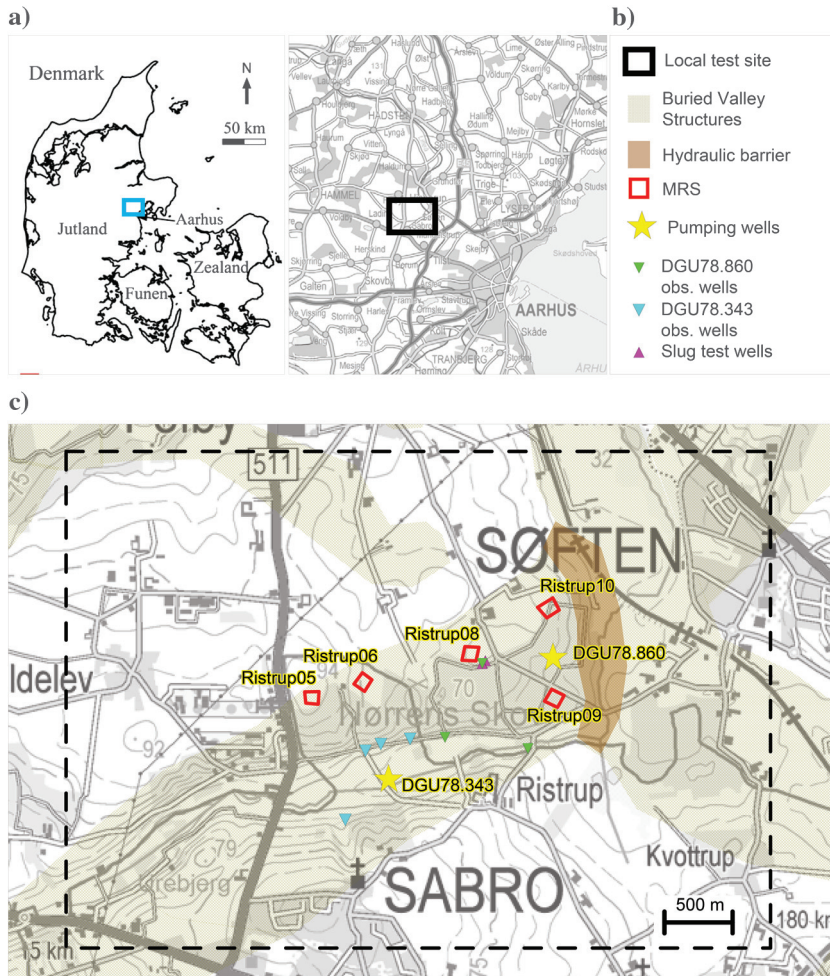


Figure 1. Field site used in the study.

water table was estimated from data curves and not based on the volume of the slug. The length of the well screens was determined from the borehole logs to 3 m. Based on the analysis, K_{eff} of the upper part of the aquifer (DGU78.779) was estimated to be 1.54×10^{-4} m/s, whereas the K_{eff} was 1.01×10^{-4} m/s for the deeper part of the aquifer (DGU78.776). The standard deviation of the estimated K_{eff} was determined from the repeated experiments in each well. This gave a standard deviation for $\log(K_{eff})$ of 0.12 for DGU78.776 and 0.10 for DGU78.779, respectively.

MRS parameter analysis

Figure 4 shows fitted FID for the MRS Ristrup09. The fitted decays include the optimal model from the least-squares nonlinear inversion and those obtained using NSMC simulation. In total, 1170 out of 2000 parameter sets were selected as behavioral in the NSMC analysis of Ristrup09, in which behavioral was defined as an objective function value less than 322. In general, there is a good agreement between simulations and observations, and only a slight bias is seen for pulse moments Q15 and Q16. This bias could have been avoided by setting up the inversion as a five-layer structure. The difference between the overall model structure obtained by using five instead of four layers was, however, limited, and we still obtained a two-aquifer system with a subdivision of the aquitard into two layers with similar parameter estimates. However, the five-layer structure resulted in increased

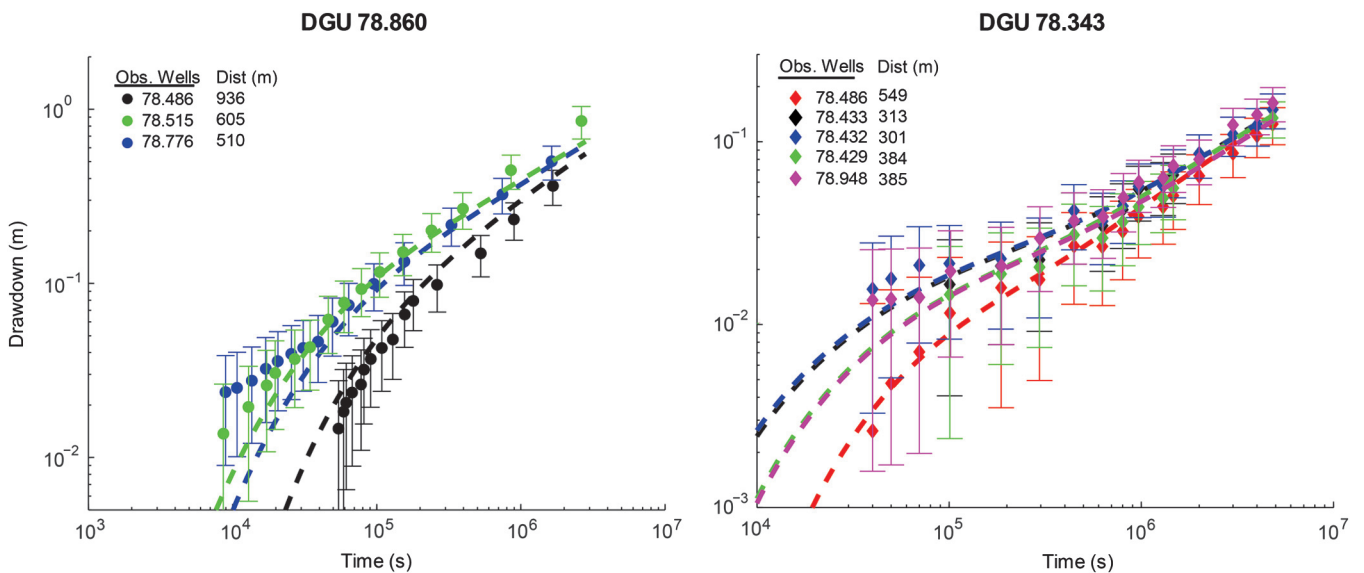


Figure 2. Results from aquifer test interpretations.

parameter uncertainty, and we, therefore, decided to use the four-layer structure in the analysis.

Figure 5 shows the parameter distributions used to generate the results shown on Figure 4. Because the bottom of the system is located at a depth of up to 120 m, the MRS method cannot reach the aquifer bottom. We therefore chose to simulate the last two layers of the MRS model as one resulting in a three-layer model for water content and decay time and a four-layer model for resistivity. It is thereby assumed that the aquifer is vertically homogeneous. Primarily based on the resistivity values, the results indicate a two-aquifer system with an upper unconfined aquifer from terrain down to 10 m below terrain and a lower primary aquifer from approximately 20 m down to approximately 120 m below terrain. It is also evident from the resistivity curve that there is a correlation between resistivity and layer thickness for layer two. Parameter values for water content and decay time for the upper two layers appear to be poorly determined. This is likely caused by limited water content and thereby signal. This is supported by the relative high resistivity observed for this layer and the low signal for small pulse moments. For the present analysis, this is, however, insignificant because the parameter estimates of the deep aquifer (layer 3) are the main target.

Figure 6 shows the parameter distributions for MRS Ristrup08 together with a simplified version of the well log from DGU78.776 located at a distance of approximately 50 m from the southeast corner of the main loop. From the two wells DGU78.776 and DGU78.779, we know that there is an upper confining clay layer and there are an upper and a deeper sand layer (aquifer) separated by a clay layer (aquitard). The clay layer near terrain can be observed in the decay time curve, which shows a fast decay and unresolved water content. The two aquifers can be observed as layers with slightly higher decay time and better resolved water content. As expected, the clayey aquitard cannot be resolved due to its small thickness. Below 60 m, there is an indication of an additional aquifer. However, this is highly uncertain because the depth of investigation is approached and because no validation data from boreholes are available. A close look at the NSMC results presented in Figure 6 indicates parameter correlations. This is seen as gradual changes between layers in the NSMC results. For the resistivity, there is correlation between layers 1 and 2 (depth interval 10–15 m), layers 3 and 4 (depth interval 55–65 m), and layers 4 and 5 (depth interval 90–100 m). For the water content, there is correlation between layers 2 and 3 (depth interval 20–35 m). The pattern is more ambiguous for the decay time distribution.

Analysis of MRS transmissivity uncertainty

We used equation 11 to calculate the combined uncertainty pertaining to the MRS parameters for all soundings. Table 2 summarizes the results. In general, there is a good agreement between the linear analysis and the nonlinear analysis. The only exception is Ristrup09, in which the nonlinear analysis estimates a variance of the MRS parameters that is significantly higher than for the linear analysis.

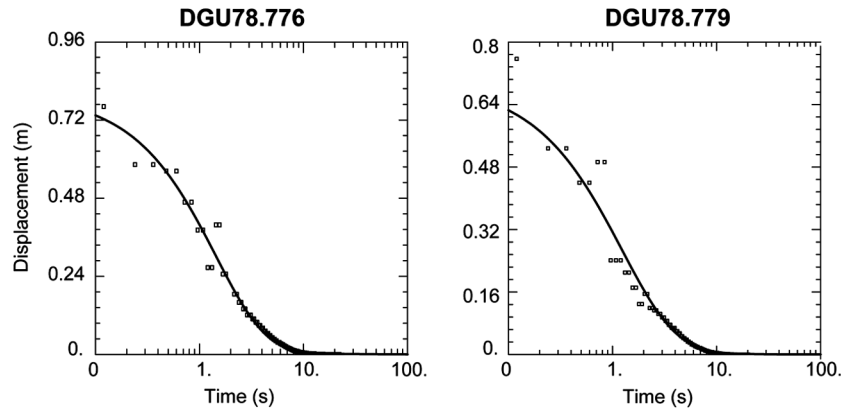


Figure 3. Examples of slug test data with fitted type curves. The slug tests were performed in two close boreholes screening the upper (DGU78.779 – 34–37 m below terrain) and the deeper (DGU78.776 – 47–50 m below terrain) part of the aquifer, respectively (see Figure 6).

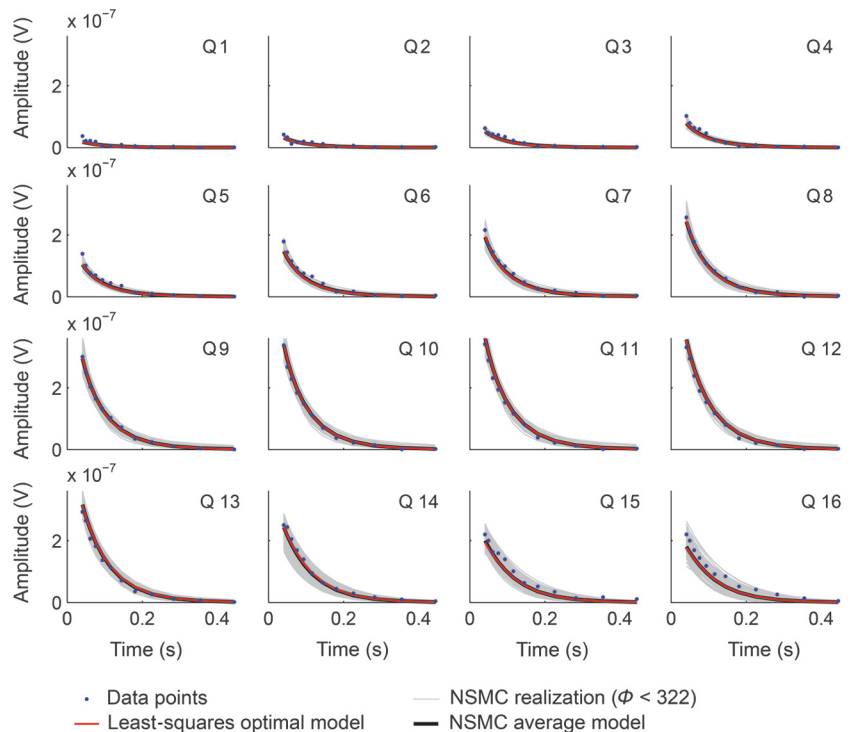


Figure 4. Example of data fit with NSMC-analysis and nonlinear inversion (Ristrup09).

To determine the transmissivity estimates derived from MRS, the C_p correlation factor must be known. This is estimated by correlation between $w * (T_2^*)^2 * lt$ and T_{HYD} data using equation 14. To take into account the spatial variability of the aquifer thickness, local estimates of T_{HYD} have been determined at each MRS sounding location. For the aquifer test data sets, this was done by calculating K_{eff} at the pumping well based on the aquifer thickness obtained from the borehole log, K_{eff} was subsequently used to calculate T_{HYD} at the MRS sites by multiplying K_{eff} with the thickness obtained from the linear analysis of the geophysical data.

Due to the local estimates of K_{eff} obtained from slug test, these results are only used for correlation to the Ristrup08 results (at a distance of 50 m). The slug-test transmissivity values were determined by multiplying the hydraulic conductivity estimates with the thickness of the aquifer estimated (see Figure 6). For aquifer 1, this was determined based on the borehole information. For aquifer 2, the thickness was determined from the joint geophysical inversion because the borehole does not penetrate to the bottom of the aquifer.

Figure 7 shows the estimated transmissivities with corresponding uncertainties. There is a general good agreement between the transmissivities estimated by two methods, and only for Ristrup10 and Ristrup08 one or both of their 95% confidence intervals do not contain the identity line with their uncertainties. Based on the correlation, it can be seen that soundings with a combination of low uncertainty for the MRS results and the hydraulic test results have a high weight in the determination of C_p (seen by the closeness of Ristrup05 and Ristrup06 to the identity line in Figure 7). Only in one case, the estimate T_{MRS} has lower uncertainty than the corresponding estimate T_{HYD} (Ristrup10). This can happen when T_{HYD} has high uncertainty whereas the estimated MRS parameters have low uncertainty. However, this is limited by the availability of hydraulic data with low uncertainty elsewhere in the data set, which can be used to reduce the uncertainty of the estimated C_p factor. The

figure also shows estimated C_p factors with pertaining uncertainties.

Figure 8 shows the estimated transmissivities with pertaining uncertainties under the assumption that parameter correlation can be ignored. In general, an increase in uncertainty can be observed, as expected. However, the degree of increase is quite variable, and for some soundings, there appears to be no effect from parameter correlation. This can be exemplified by comparing the linear estimates obtained from Ristrup06 and Ristrup09. The correlation matrix (not shown) from Ristrup06 indicates high parameter correlation among layer thickness, water content, and decay time for the aquifer. This means that these parameters cannot be determined independently and ignoring the parameter correlation increases the uncertainty of the estimated transmissivity significantly. The corresponding correlation matrix for Ristrup09 shows only limited correlation between the same parameters for the aquifer, and excluding the covariance from the analysis has limited effect on the estimated uncertainty of T_{MRS} .

DISCUSSION

Having a well-defined methodology to estimate uncertainties of MRS-derived transmissivities is important for the further usage of MRS in hydrological modeling. When such estimates are available, prior information on transmissivities from MRS can be properly weighted in hydrological model calibration or prediction uncertainty analysis in a similar fashion as often used for hydrological data (e.g., hydraulic heads and stream flows). We have therefore suggested application of a data-driven methodology to estimate uncertainties of MRS-derived transmissivities. Contrary to previously used and published methods, this methodology takes into account uncertainties related to the geophysical and the hydrological data sets and how the uncertainties propagate through the chosen petro-

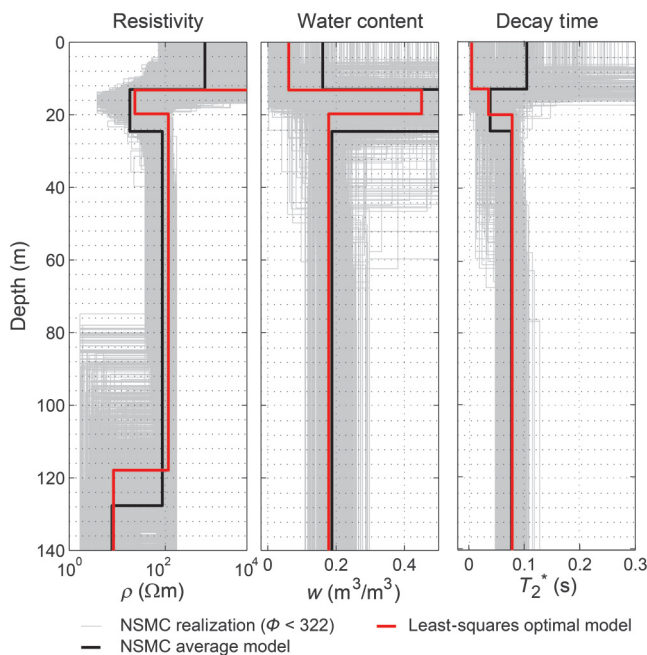


Figure 5. Parameter estimation obtained from MRS and TEM at Ristrup09. The plotted NSMC curves are for behavioral models resulting in objective function values less than 322.

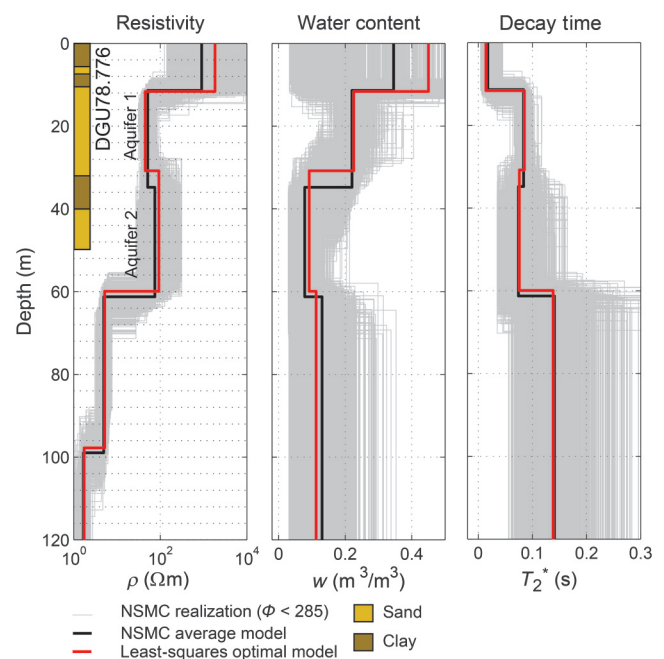


Figure 6. Parameter realizations for two aquifers system (Ristrup08).

physical relation. Using the proposed methodology for our field study, we find that in most cases, estimates of transmissivity obtained from MRS will have a higher uncertainty than the corresponding hydraulically estimated transmissivities. Based on the analysis of equations 10 to 13, this is a logical consequence because the uncertainty of the hydrological data set propagates through calibration of the correlation factor in the petrophysical relation. However, in cases where multiple hydraulic data sets are used and where some are associated with low uncertainty and others with high uncertainty, the estimated uncertainty of the C_p parameter may be low. Combining a well-estimated C_p parameter with MRS parameters with similar low uncertainty will thereby result in low uncertainty of the derived T_{MRS} . If the sounding resulting in such a T_{MRS} estimate is located close to hydraulic data set of high uncertainty, the uncertainty of T_{MRS} may be the smallest. Such a special case was present for a single sounding in our field case, and the results can be seen from Figure 7. However, in the general case with uniform uncertainty on T_{HYD} , the uncertainty of T_{MRS} will always exceed the corresponding T_{HYD} uncertainties due to the uncertainty of the geophysical parameters as well as of the correlation factor.

We have suggested a methodology to estimate the uncertainty of the C_p parameter. However, the literature contains multiple references to studies where these correlation factors have been estimated for different types of lithology (e.g., Legchenko et al., 2002; Vouillamoz et al., 2007; Mohnke and Yaramanci, 2008; Plata and Rubio, 2008; Ryom Nielsen et al., 2011). Provided reasonable uncertainty estimates of these factors for various types of deposits can be estimated, they can be used in combination with equation 10 in areas with no or limited hydrological data. Without having made the analysis, it is though our expectation that this will result in C_p factors with high uncertainty that will propagate through to the estimated T_{MRS} . This may however change in the future with increasing experience on the ranges of the C_p factor.

To take into account the effect of parameter correlations in the analysis, the full covariance matrix of the joint TEM and MRS inversion problem needs to be estimated. This is needed due to the complex parameter correlation pattern observed in the present analysis. Parameters can thereby be correlated with layer thick-

nesses (in cases where TEM cannot resolve the layer boundaries) and to parameters pertaining to layers below and above the target aquifer. This means that the effect of disregarding parameter correlation will be different depending on the local geologic structure. In some cases, ignoring parameter correlation will increase the uncertainty of the derived transmissivities significantly, making the estimate conservative, whereas in other cases (in which parameter correlations are less profound), the effect will be negligible.

For the field case studied here, we find that the linear and a nonlinear estimates of the parameter variance/covariance matrix are similar, thereby resulting in similar uncertainty estimates for the derived T_{MRS} . Due to the linearity of the MRS forward problem, we expect this to be similar for other field sites; however, our basis for this argument is small given our limited data set. We therefore advocate for making further analysis of the contribution to parameter uncertainty from nonlinear analysis, e.g., based on a full MCMC

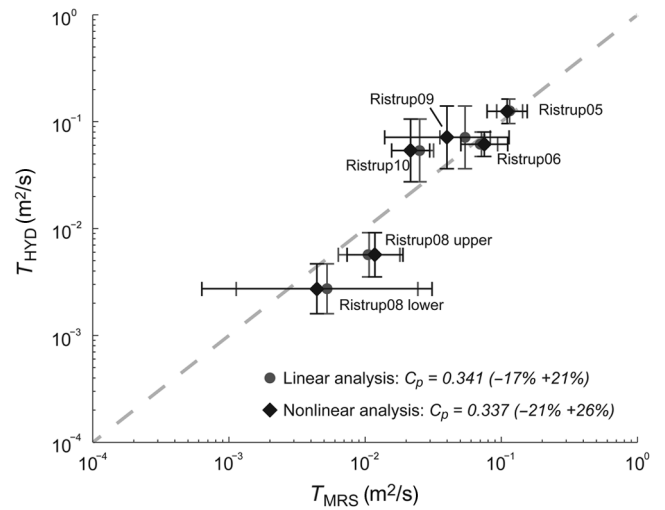


Figure 7. Transmissivity estimates with uncertainties (95% confidence intervals). Estimated C_p values are shown with upper and lower 95% confidence intervals given in the parenthesis.

Table 2. Results from the uncertainty analysis of the MRS parameters comparing the linear and nonlinear analyses. The second and fifth columns show the product of the terms pertaining to the geophysical parameters (from the linear and nonlinear analyses, respectively). The third and sixth columns show the variance of the products in which covariance is included into the analysis, and the fourth and seventh columns show the variance of the product if covariance is ignored.

Sounding/hyd. data set	$w * (T_2^*)^2 * l$	Linear analysis		Nonlinear analysis		
		With covariance $\text{var}(\log(w * (T_2^*)^2 * l))$	Without covariance $\text{var}(\log(w * (T_2^*)^2 * l))$	mean($w * (T_2^*)^2 * l$)	With covariance $\text{var}(\log(w * (T_2^*)^2 * l))$	Without covariance $\text{var}(\log(w * (T_2^*)^2 * l))$
Ristrup05/DGU78.343	0.338	5.9E - 04	1.3E - 03	0.328	3.0E - 03	1.0E - 02
Ristrup06/DGU78.343	0.210	1.9E - 03	2.6E - 02	0.223	5.0E - 03	3.0E - 02
Ristrup08 Upper/ DGU78.779	0.031	1.1E - 02	2.1E - 02	0.035	8.3E - 03	2.2E - 02
Ristrup08 Lower/ DGU78.776	0.015	1.1E - 01	6.2E - 02	0.013	1.8E - 01	1.3E - 01
Ristrup09/DGU78.860	0.159	7.1E - 03	9.0E - 03	0.118	5.1E - 02	5.1E - 02
Ristrup10/DGU78.860	0.074	9.7E - 04	2.9E - 03	0.064	2.4E - 03	4.2E - 03

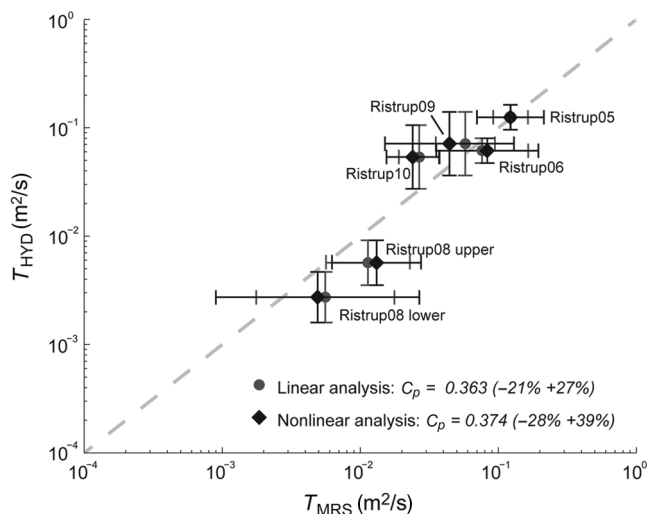


Figure 8. Estimated transmissivities with uncertainties (95% confidence intervals), under the assumption that parameter covariance can be ignored. Estimated C_p values are shown with upper and lower 95% confidence intervals given in the parentheses.

analysis. Should future analysis of the uncertainty show that linear and nonlinear uncertainty estimates are similar, the uncertainty estimation method presented would benefit by making it much more computationally efficient, due to the limited computational effort needed to estimate the linear estimate of the parameter covariance matrix.

CONCLUSION

In this study, we have proposed an equation that can be used for estimating the uncertainty of MRS estimated transmissivities (T_{MRS}). The estimate takes into account important factors such as input parameter uncertainty and parameter correlations. These input parameters originate from analysis of geophysical and hydrological data that have an inherent uncertainty. This uncertainty needs to be propagated through the petrophysical relation to produce a reliable uncertainty estimate for T_{MRS} . Because the petrophysical relation needs to be calibrated to transmissivities (T_{HYD}) estimated from available uncertain hydrological data sets, this will in most cases result in higher uncertainty for T_{MRS} than for the corresponding T_{HYD} .

We have also compared the uncertainty estimates of the geophysical parameters by performing a linear and a nonlinear uncertainty analyses. In this study, we found that the parameter uncertainty obtained by the nonlinear analysis was slightly higher than that obtained by the linear analysis. However, due to our limited data set, it is difficult to draw any general conclusions and we advocate for further analysis of this problem.

Based on crosscorrelation between T_{MRS} and T_{HYD} , we have proposed a method to estimate the uncertainty of the correlation factor in the petrophysical relation. This methodology takes into account that the input can have variable uncertainty and that the largest weight should therefore be given to data with the least uncertainty. Other methods to estimate the correlation factor exist, and the literature holds multiple references. In areas with limited hydrological data, it is therefore expected that T_{MRS} can be estimated using these literature values as long as the uncertainty is propagated correctly

through the petrophysical relation, by adding the corresponding uncertainty to the correlation factor and by using the equations derived in the present study.

ACKNOWLEDGMENTS

This study was financed by the HyGEM project “Integrating geophysics, geology, and hydrology for improved groundwater and environmental management,” project no. 11-116763. The funding for HyGEM is provided by the Danish Council for Strategic Research. The authors would also like to acknowledge the contribution made by three anonymous reviewers. Their valuable comments greatly improved the content and readability of the manuscript. The authors would also like to acknowledge A. A. Behroozmand and J. J. Larsen for fruitful discussions on the interpretation and the noise processing made of the MRS data. Finally, we would like to acknowledge master student S. Rejker and Ph.D. student P. Aa. Marker for assisting with the data collection of MRS data and slug test data, respectively.

REFERENCES

- Aarhus Geophysics, 2014, Processing and inversion of SkyTEM data: Kasted and Truelsenbjerg, Aarhus Geophysics, 108.
- Anderson, M. P., W. W. Woessner, and R. J. Hunt, 2015, Applied groundwater modeling: Elsevier Inc.
- Aster, R. C., B. Borchers, and C. H. Thurber, 2005, Parameter estimation and inverse problems: Elsevier Academic Press.
- Auken, E., A. V. Christiansen, C. Kirkegaard, G. Fiandaca, C. Schamper, A. A. Behroozmand, A. Binley, E. Nielsen, F. Effersø, N. B. Christensen, K. I. Sørensen, N. Foged, and G. Vignoli, 2014, An overview of a highly versatile forward and stable inverse algorithm for airborne, ground-based and borehole electromagnetic and electric data: *Exploration Geophysics*, **46**, 223–235, doi: [10.1071/EG13097](https://doi.org/10.1071/EG13097).
- Bear, J., 1988, Dynamics of fluids in porous media: Dover Publication Inc.
- Behroozmand, A. A., E. Auken, G. Fiandaca, and A. V. Christiansen, 2012a, Improvement in MRS parameter estimation by joint and laterally constrained inversion of MRS and TEM data: *Geophysics*, **77**, no. 4, WB191–WB200, doi: [10.1190/geo2011-0404.1](https://doi.org/10.1190/geo2011-0404.1).
- Behroozmand, A. A., E. Auken, G. Fiandaca, A. V. Christiansen, and N. B. Christensen, 2012b, Efficient full decay inversion of MRS data with a stretched-exponential approximation of the T_2^* distribution: *Geophysical Journal International*, **190**, 900–912, doi: [10.1111/j.1365-246X.2012.05558.x](https://doi.org/10.1111/j.1365-246X.2012.05558.x).
- Behroozmand, A. A., K. Keating, and E. Auken, 2015, A review of the principles and applications of the NMR technique for near-surface characterization: *Surveys in Geophysics*, **36**, 27–85, doi: [10.1007/s10712-014-9304-0](https://doi.org/10.1007/s10712-014-9304-0).
- Blæsberg, H. J., 2006, Opstilling af grundvandsmodel for Ristrup Kildepladsud fra geologiske og geofysiske data samt kalibrering ved hydrologiske og hydrauliske data: M.S. thesis, Department of Geoscience, Aarhus University.
- Boucher, M., G. Favreau, J. M. Vouillamoz, Y. Nazoumou, and A. Legchenko, 2009, Estimating specific yield and transmissivity with magnetic resonance sounding in an unconfined sandstone aquifer (Niger): *Hydrogeology Journal*, **17**, 1805–1815, doi: [10.1007/s10040-009-0447-x](https://doi.org/10.1007/s10040-009-0447-x).
- Butler, J. J., 1998, The design, performance and analysis of slug tests: Lewis Publishers.
- Butler, J. J., and Z. L. Wenzhi, 1991, Pumping tests in non-uniform aquifers — The linear strip case: *Journal of Hydrology*, **128**, 69–99, doi: [10.1016/0022-1694\(91\)90132-2](https://doi.org/10.1016/0022-1694(91)90132-2).
- Chalikakis, K., M. R. Nielsen, and A. Legchenko, 2008, MRS applicability for a study of glacial sedimentary aquifers in Central Jutland, Denmark: *Journal of Applied Geophysics*, **66**, 176–187, doi: [10.1016/j.jappgeo.2007.11.005](https://doi.org/10.1016/j.jappgeo.2007.11.005).
- Dalgaard, E., 2014, Development of efficient noise cancellation techniques for SNMR Data: Ph.D. thesis, Aarhus University.
- Dalgaard, E., E. Auken, and J. J. Larsen, 2012, Adaptive noise cancelling of multichannel magnetic resonance sounding signals: *Geophysical Journal International*, **191**, 88–100, doi: [10.1111/j.1365-246X.2012.05618.x](https://doi.org/10.1111/j.1365-246X.2012.05618.x).
- Dlubac, K., R. Knight, and K. Keating, 2014, A numerical study of the relationship between NMR relaxation and permeability in sands and gravels: *Near Surface Geophysics*, **12**, 219–230, doi: [10.3997/1873-0604.2013042](https://doi.org/10.3997/1873-0604.2013042).

- Dlugosch, R., T. Günther, M. Müller-Petke, and U. Yaramanci, 2013, Improved prediction of hydraulic conductivity for coarse-grained, unconsolidated material from nuclear magnetic resonance: *Geophysics*, **78**, no. 4, EN55–EN64, doi: [10.1190/geo2012-0187.1](https://doi.org/10.1190/geo2012-0187.1).
- Doherty, J., 2003, Ground water model calibration using pilot points and regularization: *Ground Water*, **41**, 170–177, doi: [10.1111/j.1745-6584.2003.tb02580.x](https://doi.org/10.1111/j.1745-6584.2003.tb02580.x).
- Doherty, J., 2010, PEST model-independent parameter estimation user manual (5th ed.): Watermark Numerical Computing.
- Fienen, M. N., C. T. Muffels, and R. J. Hunt, 2009, On constraining pilot point calibration with regularization in PEST: *Groundwater*, **47**, 835–844, doi: [10.1111/j.1745-6584.2009.00579.x](https://doi.org/10.1111/j.1745-6584.2009.00579.x).
- Grunewald, E., and R. Knight, 2011, The effect of pore size and magnetic susceptibility on the surface NMR relaxation parameter T_2^* : *Near Surface Geophysics*, **9**, 169–178, doi: [10.3997/1873-0604.2010062](https://doi.org/10.3997/1873-0604.2010062).
- Günther, T., and M. Müller-Petke, 2012, Hydraulic properties at the North Sea island of Borkum derived from joint inversion of magnetic resonance and electrical resistivity soundings: *Hydrology and Earth System Sciences*, **16**, 3279–3291, doi: [10.5194/hess-16-3279-2012](https://doi.org/10.5194/hess-16-3279-2012).
- Harbaugh, A. W., 2005, MODFLOW-2005 — The U.S. Geological Survey Modular Ground-Water Model — The Ground-Water Flow Process: U.S. Geological Survey Techniques and Methods 6-A16.
- Hunt, R. J., J. Doherty, and M. Tonkin, 2007, Are models too simple? Arguments for increased parameterization: *Ground Water*, **45**, 254–262, doi: [10.1111/j.1745-6584.2007.00316.x](https://doi.org/10.1111/j.1745-6584.2007.00316.x).
- Jørgensen, F., and P. B. E. Sandersen, 2006, Buried and open tunnel valleys in Denmark-erosion beneath multiple ice sheets: *Quaternary Science Reviews*, **25**, 1339–1363, doi: [10.1016/j.quascirev.2005.11.006](https://doi.org/10.1016/j.quascirev.2005.11.006).
- Kenyon, W. E., P. I. Day, C. Straley, and J. F. Willemsen, 1988, Three-part study of NMR longitudinal relaxation properties of water-saturated sandstones: *SPE Formation Evaluation*, **3**, 622–636, doi: [10.2118/15643-PA](https://doi.org/10.2118/15643-PA).
- Kruseman, G. P., and N. A. de Ridder, 2000, Analysis and Evaluation of Pumping Test Data: International Institute for Land Reclamation and Improvement.
- Larsen, J. J., E. Dalgaard, and E. Auken, 2014, Noise cancelling of MRS signals combining model-based removal of powerline harmonics and multichannel Wiener filtering: *Geophysical Journal International*, **196**, 828–836, doi: [10.1093/gji/ggt422](https://doi.org/10.1093/gji/ggt422).
- Legchenko, A., J. M. Baltassat, A. Beauce, and J. Bernard, 2002, Nuclear magnetic resonance as a geophysical tool for hydrogeologists: *Journal of Applied Geophysics*, **50**, 21–46, doi: [10.1016/S0926-9851\(02\)00128-3](https://doi.org/10.1016/S0926-9851(02)00128-3).
- Legchenko, A., J. M. Baltassat, A. Bobachev, C. Martin, H. Robain, and J. M. Vouillamoz, 2004, Magnetic resonance sounding applied to aquifer characterization: *Ground Water*, **42**, 363–373, doi: [10.1111/j.1745-6584.2004.tb02684.x](https://doi.org/10.1111/j.1745-6584.2004.tb02684.x).
- Legchenko, A., and P. Valla, 2002, A review of the basic principles for proton magnetic resonance sounding measurements: *Journal of Applied Geophysics*, **50**, 3–19, doi: [10.1016/S0926-9851\(02\)00127-1](https://doi.org/10.1016/S0926-9851(02)00127-1).
- Lubczynski, M. W., and J. Roy, 2007, Use of MRS for hydrological system parameterization and modeling: *Boletín Geológico y Minero*, **118**, 509–530.
- Mohnke, O., and U. Yaramanci, 2008, Pore size distributions and hydraulic conductivities of rocks derived from magnetic resonance sounding relaxation data using multi-exponential decay time inversion: *Journal of Applied Geophysics*, **66**, 73–81, doi: [10.1016/j.jappgeo.2008.05.002](https://doi.org/10.1016/j.jappgeo.2008.05.002).
- Møller, I., V. H. Søndergaard, and F. Jørgensen, 2009, Geophysical methods and data administration in Danish groundwater mapping: Geological Survey of Denmark and Greenland Bulletin, **17**, 41–44.
- Plata, J. L., and F. M. Rubio, 2008, The use of MRS in the determination of hydraulic transmissivity: The case of alluvial aquifers: *Journal of Applied Geophysics*, **66**, 128–139, doi: [10.1016/j.jappgeo.2008.04.001](https://doi.org/10.1016/j.jappgeo.2008.04.001).
- Ryom Nielsen, M., T. F. Hagensen, K. Chalikakis, and A. Legchenko, 2011, Comparison of transmissivities from MRS and pumping tests in Denmark: *Near Surface Geophysics*, **9**, 211–223, doi: [10.3997/1873-0604.2010071](https://doi.org/10.3997/1873-0604.2010071).
- Sørensen, K. I., and E. Auken, 2004, SkyTEM — A new high-resolution helicopter transient electromagnetic system: *Exploration Geophysics*, **35**, 191–199.
- Theis, C. V., 1935, The relation between the lowering of the piezometric surface and the rate and duration of discharge of a well using groundwater storage: *Eos Transactions American Geophysical Union*, **16**, 519–524, doi: [10.1029/TR016i002p00519](https://doi.org/10.1029/TR016i002p00519).
- Tonkin, M., and J. Doherty, 2009, Calibration-constrained Monte Carlo analysis of highly parameterized models using subspace techniques: *Water Resources Research*, **45**, W00B10, doi: [10.1029/2007WR006678](https://doi.org/10.1029/2007WR006678).
- van der Kamp, G., and H. Maathuis, 2012, The unusual and large drawdown response of buried-valley aquifers to pumping: *Ground Water*, **50**, 207–215, doi: [10.1111/j.1745-6584.2011.00833.x](https://doi.org/10.1111/j.1745-6584.2011.00833.x).
- Vandenberg, A., 1977, Type curves for analysis of pump tests in leaky strip aquifers: *Journal of Hydrology*, **33**, 15–26, doi: [10.1016/0022-1694\(77\)90095-6](https://doi.org/10.1016/0022-1694(77)90095-6).
- Vilhelmsen, T. N., A. A. Behroozmand, S. Christensen, and T. H. Nielsen, 2014, Joint inversion of aquifer test, MRS and TEM data: *Water Resources Research*, **50**, 3956–3975, doi: [10.1002/2013WR014679](https://doi.org/10.1002/2013WR014679).
- Vouillamoz, J., J. M. Baltassat, J. F. Girard, J. Plata, and A. Legchenko, 2007, Hydrogeological experience in the use of MRS: *Boletín Geológico y Minero*, **118**, 531–550.